

93. Dynamical Electroweak Symmetry Breaking: Implications of the H^0

Revised August 2019 by K.M. Black (Wisconsin U.), R.Sekhar Chivukula (UC San Diego) and M. Narain (Brown U.).

93.1 Introduction and Phenomenology

In theories of dynamical electroweak symmetry breaking, the electroweak interactions are broken to electromagnetism by the vacuum expectation value of a composite operator, typically a fermion bilinear. In these theories, the longitudinal components of the massive weak bosons are identified with composite Nambu-Goldstone bosons arising from dynamical symmetry breaking in a strongly-coupled extension of the standard model. Viable theories of dynamical electroweak symmetry breaking must also explain (or at least accommodate) the presence of an additional composite scalar state to be identified with the H^0 scalar boson [1, 2] – a state unlike any other observed previously.

Theories of dynamical electroweak symmetry breaking can be classified by the nature of the composite singlet state to be associated with the H^0 and the corresponding dimensional scales f , the analog of the pion decay-constant in QCD, and Λ , the scale of the underlying strong dynamics.¹ Of particular importance is the ratio v/f , where $v^2 = 1/(\sqrt{2}G_F) \approx (246 \text{ GeV})^2$, since this ratio measures the expected size of the deviations of the couplings of a composite Higgs boson from those expected in the standard model. The basic possibilities, and the additional states that they predict, are described below.

93.1.1 Technicolor, $v/f \simeq 1$, $\Lambda \simeq 1 \text{ TeV}$

Technicolor models [7–9] provided the first examples of theories of dynamical electroweak symmetry breaking. These theories incorporate a new asymptotically free gauge theory (“technicolor”) and additional massless fermions (“technifermions” transforming under a vectorial representation of the gauge group). The global chiral symmetry of the fermions is spontaneously broken by the formation of a technifermion condensate, just as the approximate chiral symmetry in QCD is broken down to isospin by the formation of a quark condensate. The $SU(2)_W \times U(1)_Y$ interactions are embedded in the global technifermion chiral symmetries in such a way that the only unbroken gauge symmetry after chiral symmetry breaking is $U(1)_{em}$.² The theories naturally provide the Nambu-Goldstone bosons “eaten” by the W and Z boson. There would also typically be additional heavy states (e.g. vector mesons, analogous to the ρ and ω mesons in QCD) with TeV masses [13, 14], and the WW and ZZ scattering amplitudes would be expected to be strong at energies of order 1 TeV.

There are various possibilities for the scalar H^0 in technicolor models. First, the H^0 could be identified as a singlet scalar resonance, analogous to the σ particle expected in pion-scattering in QCD [15, 16]. Alternatively, the H^0 could be identified as a dilaton, a (pseudo-)Goldstone boson of scale invariance in theories of “walking technicolor” [17–21].³ Finally, the H^0 could be identified as an additional isosinglet state if the chiral symmetry breaking pattern of the technicolor theory provides for such a state.⁴ In all of these cases, however, one expects large deviations in

¹In a strongly interacting theory “Naive Dimensional Analysis” [3, 4] implies that, in the absence of fine-tuning, $\Lambda \simeq g^* f$ where $g^* \simeq 4\pi$ is the typical size of a strong coupling in the low-energy theory [5, 6]. This estimate is modified in the presence of multiple flavors or colors [7].

²For a review of technicolor models, see [10–12].

³If both the electroweak symmetry and the approximate scale symmetry are broken only by electroweak doublet condensate(s), then the decay-constants for scale and electroweak symmetry breaking may be approximately equal – differing only by terms formally proportional to the amount of explicit scale-symmetry breaking.

⁴In this case, however, the coupling strength of the singlet state to WW and ZZ pairs would be comparable

the couplings of this particle from those of the standard model Higgs boson. Since the couplings observed for the H^0 approximate those of the Higgs boson to the 10% level, models of this kind are very highly constrained.

93.1.2 The Higgs doublet as a pseudo-Nambu-Goldstone Boson, $v/f < 1$, $\Lambda > 1$ TeV

In technicolor models, the symmetry-breaking properties of the underlying strong dynamics necessarily breaks the electroweak gauge symmetries. An alternative possibility is that the underlying strong dynamics itself does not break the electroweak interactions, and that the entire quartet of bosons in the Higgs doublet (including the state associated with the H^0) are composite (pseudo-) Nambu-Goldstone particles [23,24]. In this case, the underlying dynamics can occur at energies exceeding 1 TeV and additional interactions with the top-quark mass generating sector (and possibly with additional weakly-coupled gauge bosons) cause the vacuum energy to be minimized when the composite Higgs doublet gains a vacuum expectation value [25,26]. In these theories, the couplings of the remaining singlet scalar state would naturally be equal to that of the standard model Higgs boson up to corrections of order $(v/f)^2$ and, therefore, constraints on the size of deviations of the H^0 couplings from that of the standard model Higgs [27] give rise to lower bounds on the scales f and Λ .⁵

The electroweak gauge interactions, as well as the interactions responsible for the top-quark mass, explicitly break the chiral symmetries of the composite Higgs model and lead generically to sizable corrections to the mass-squared of the Higgs-doublet – the so-called “Little Hierarchy Problem” [28]. “Little Higgs” theories [29–32] are examples of composite Higgs models in which the (collective) symmetry-breaking structure is selected so as to suppress these contributions to the Higgs mass-squared.

Composite Higgs models typically require a larger global symmetry of the underlying theory, and hence additional relatively light (compared to Λ) scalar particles, extra electroweak vector bosons (e.g. an additional $SU(2) \times U(1)$ gauge group), and vector-like partners of the top-quark of charge $+2/3$ and possibly also $+5/3$ [33]. In addition to these states, one would expect the underlying dynamics to yield additional scalar and vector resonances with masses of order Λ . If the theory respects a custodial symmetry [34], the couplings of these additional states to the electroweak and Higgs boson will be related – and, for example, one might expect a charged vector resonance to have similar branching ratios to WZ and WH . Different composite Higgs models utilize different mechanisms for arranging for the hierarchy of scales $v < f$ and arranging for a scalar Higgs self-coupling small enough to produce an H^0 of mass of order 125 GeV, for a review see [35]. If the additional states in these models carry color, they can provide additional contributions to Higgs production via gluon fusion [36]. The extent to which Higgs production at the LHC conforms with standard model predictions provides additional constraints (typically lower bounds on the masses of the additional colored states of order 0.7 TeV) on these models.

In addition, if the larger symmetry of the underlying composite Higgs theory does not commute with the standard model gauge group, then the additional states found in those models – especially those related to the top-quark, which tend to have the largest couplings to the electroweak sector – may be *colorless*. For example, in twin Higgs models [37], the top-partners carry no standard model charges. The phenomenology of the additional states in twin Higgs theories is rather different, since to the couplings to gluon and photon pairs, and these would all arise from loop-level couplings in the underlying technicolor theory [22].

⁵In these models v/f is an adjustable parameter, and in the limit $v/f \rightarrow 1$ they reduce, essentially, to the technicolor models discussed in the previous subsection. Our discussion here is consistent with that given there, since we expect corrections to the SM Higgs couplings to be large for $v/f \simeq 1$. Current measurements constrain the couplings of the H^0 to equal those predicted for the Higgs in the standard model to about the 10% level [27], suggesting that f must have values of order a TeV or higher and, therefore, a dynamical scale Λ of at least several TeV.

lacking color the production of these particles at the LHC will be suppressed – and, their decays may occur only via the electroweak symmetry breaking sector, leading to their being long-lived.

93.1.3 *Top-Condensate, Top-Color, Top-Seesaw and related theories, $v/f < 1$, $\Lambda > 1$ TeV*

A final alternative is to consider a strongly interacting theory with a high (compared to a TeV) underlying dynamical scale that *would* naturally break the electroweak interactions, but whose strength is adjusted (“fine-tuned”) to produce electroweak symmetry breaking at 1 TeV. This alternative is possible if the electroweak (quantum) phase transition is continuous (second order) in the strength of the strong dynamics [38]. If the fine tuning can be achieved, the underlying strong interactions will produce a light composite Higgs bound state with couplings equal to that of the standard model Higgs boson up to corrections of order $(1 \text{ TeV}/\Lambda)^2$. As in theories in which electroweak symmetry breaking occurs through vacuum alignment, therefore, constraints on the size of deviations of the H^0 couplings from that of the standard model Higgs give rise to lower bounds on the scale Λ . Formally, in the limit $\Lambda \rightarrow \infty$ (a limit which requires arbitrarily fine adjustment of the strength of the high-energy interactions), these theories are equivalent to a theory with a fundamental Higgs boson – and the fine adjustment of the coupling strength is a manifestation of the hierarchy problem of theories with a fundamental scalar particle.

In many of these theories the top-quark itself interacts strongly (at high energies), potentially through an extended color gauge sector [39, 39–43]. In these theories, top-quark condensation (or the condensation of an admixture of the top with additional vector-like quarks) is responsible for electroweak symmetry breaking, and the H^0 is identified with a bound state involving the third generation of quarks. These theories typically include an extra set of massive color-octet vector bosons (top-gluons), and an extra $U(1)$ interaction (giving rise to a top-color Z') which couple preferentially to the third generation and whose masses define the scale Λ of the underlying physics.

93.1.4 *Flavor*

In addition to the electroweak symmetry breaking dynamics described above, which gives rise to the masses of the W and Z particles, additional interactions must be introduced to produce the masses of the standard model fermions. Two general avenues have been suggested for these new interactions. In “extended technicolor” (ETC) theories [44, 45], the gauge interactions in the underlying strongly interacting theory are extended to incorporate flavor. This extended gauge symmetry is broken down (possibly sequentially, at several different mass scales) to the residual strong interaction responsible for electroweak symmetry breaking. The massive gauge-bosons corresponding to the broken symmetries then mediate interactions between mass operators for the quarks/leptons and the corresponding bilinears of the strongly-interacting fermions, giving rise to the masses of the ordinary fermions after electroweak symmetry breaking.

In the case of “partial compositeness” [46], the additional flavor-dependent interactions arise from mixing between the ordinary quarks and leptons and massive composite fermions in the strongly-interacting underlying theory. Theories incorporating partial compositeness include additional vector-like partners of the ordinary quarks and leptons, typically with masses of order a TeV or less.

In both cases, the effects of flavor interactions on the electroweak properties of the ordinary quarks and leptons are likely to be most pronounced in the third generation of fermions.⁶ The additional particles present in these theories, especially the additional scalars, often couple more strongly to heavier fermions.

Moreover, since the flavor interactions must give rise to quark mixing, we expect that a generic

⁶Indeed, from this point of view, the vector-like partners of the top-quark in top-seesaw and little Higgs models can be viewed as incorporating partial compositeness to explain the origin of the top quark’s large mass.

theory of this kind could give rise to large flavor-changing neutral-currents [45]. In ETC theories, these constraints are typically somewhat relaxed if the theory incorporates approximate generational flavor symmetries [47], the theory has a slowly running coupling constant or “walks” [17–21], or if $\Lambda > 1$ TeV [48]. In theories of partial compositeness, the masses of the ordinary fermions depend on the scaling-dimension of the operators corresponding to the composite fermions with which they mix. This leads to a new mechanism for generating the mass-hierarchy of the observed quarks and leptons that, potentially, ameliorates flavor-changing neutral current problems and can provide new contributions to the composite Higgs potential which allow for $v/f < 1$ [49–53].

Alternatively, one can assume that the underlying flavor dynamics respect flavor symmetries (“minimal” [54, 55] or “next-to-minimal” [56] flavor violation) that suppress flavor-changing neutral currents in the two light generations. Additional considerations apply when extending these arguments to potential explanation of neutrino masses (see, for example, [57, 58]).

Since the underlying high-energy dynamics in these theories are strongly coupled, there are no reliable calculation techniques that can be applied to analyze their properties. Instead, most phenomenological studies depend on the construction of a “low-energy” effective theory describing additional scalar, fermion, or vector boson degrees of freedom, which incorporates the relevant symmetries and, when available, dynamical principles. In some cases, motivated by the AdS/CFT correspondence [59], the strongly-interacting theories described above have been investigated by analyzing a dual compactified five-dimensional gauge theory. In these cases, the AdS/CFT “dictionary” is used to map the features of the underlying strongly coupled high-energy dynamics onto the low-energy weakly coupled dual theory [60].

More recently, progress has been made in investigating strongly-coupled models using lattice gauge theory [61]. These calculations offer the prospect of establishing which strongly coupled theories of electroweak symmetry breaking have a particle with properties consistent with those observed for the H^0 – and for establishing concrete predictions for these theories at the LHC [62].

93.2 Experimental Searches

As discussed above, the extent to which the couplings of the H^0 conform to the expectations for a standard model Higgs boson constrains the viability of each of these models. Measurements of the H^0 couplings, and their interpretation in terms of effective field theory, are summarized in the H^0 review in this volume. In what follows, we will focus on searches for the additional particles that might be expected to accompany the singlet scalar: extra scalars, fermions, and vector bosons. In some cases, detailed model-specific searches have been made for the particles described above (though generally not yet taking account of the demonstrated existence of the H^0 boson).

In most cases, however, generic searches (e.g. for extra W' or Z' particles, extra scalars in the context of multi-Higgs models, or for fourth-generation quarks) are quoted that can be used – when appropriately translated – to derive bounds on a specific model of interest.

The mass scale of the new particles implied by the interpretations of the low mass of H^0 discussed above, and existing studies from the Tevatron and lower-energy colliders, suggests that only the Large Hadron Collider has any real sensitivity. A number of analyses already carried out by ATLAS and CMS use relevant final states and might have been expected to observe a deviation from standard model expectations – in no case so far has any such deviation been reported. The detailed implications of these searches in various model frameworks are described below.

Except where otherwise noted, all limits in this section are quoted at a confidence level of 95%. The searches at $\sqrt{s} = 8$ TeV (Run 1) are based on 20.3 fb^{-1} of data recorded by ATLAS, and an integrated luminosity of 19.7 fb^{-1} analyzed by CMS. The datasets collected at $\sqrt{s} = 13$ TeV during Run 2 of the LHC since 2015 are based on analyses with varied integrated luminosities ranging from $\sim 2\text{--}140 \text{ fb}^{-1}$.

93.2.1 Searches for Z' or W' Bosons

Massive vector bosons or particles with similar decay channels would be expected to arise in Little Higgs theories, in theories of Technicolor, or models involving a dilaton, adjusted to produce a light Higgs boson, consistent with the observed H^0 . These particles would be expected to decay to pairs of vector bosons, or to third generation quarks, or to leptons. The generic searches for W' and Z' vector bosons listed below can, therefore, be used to constrain models incorporating a composite Higgs-like boson.

A general review of searches for Z' and W' bosons is also included in this volume [63, 64]. In the context of the dynamical electroweak symmetry breaking models, we emphasize their decays to third generation fermions by including a detailed overview, while also briefly summarizing the other searches.

 $Z' \rightarrow \ell\ell$:

ATLAS [65] and CMS [66] have both searched for Z' production with $Z' \rightarrow ee$ or $\mu\mu$. No deviation from the standard model prediction was seen in the dielectron and dimuon invariant mass spectra, by either the ATLAS or the CMS analysis, and lower limits on possible Z' boson masses were set. A Z'_{SSM} with couplings equal to the standard model Z' (a “sequential standard model” Z') and a mass below 5.1 TeV was excluded by ATLAS, while CMS set a lower mass limit of 5.15 TeV. The experiments also place limits on the parameters of extra dimension models and in the case of ATLAS on the parameters of a minimal walking technicolor model [17–21], consistent with a 125 GeV Higgs boson [67]. For a general review of searches in these channels see the PDG review of Z prime in this volume [63].

In addition, both experiments have also searched for Z' decaying to a ditau final state [68, 69]. An excess in $\tau^+\tau^-$ could have interesting implications for models in which lepton universality is not a requirement and enhanced couplings to the third generation are allowed. This analysis led to lower limits on the mass of a Z'_{SSM} of 2.4 and 2.1 TeV from ATLAS and CMS respectively.

 $Z' \rightarrow q\bar{q}$:

The ability to relatively cleanly select $t\bar{t}$ pairs at the LHC together with the existence of enhanced couplings to the third generation in many models makes it worthwhile to search for new particles decaying in this channel. Both ATLAS [70] and CMS [71] have carried out searches for new particles decaying into $t\bar{t}$.

Both the ATLAS and CMS collaborations searched for $t\bar{t}$ in the all hadronic mode [72] [73] in both the resolved and boosted regions. No evidence of resonance production were seen and limits were produced for various models including the Z' boson in topcolor-assisted technicolor which excludes masses less than 3.1 to 3.6 TeV (ATLAS) depending on the details of the model and 3.3, 5.25, and 6.65 TeV for widths of 1, 10 and 30 percent relative to the mass of the resonance .

ATLAS also presented results on the lepton plus jets final state, where the top quark pair decays as $t\bar{t} \rightarrow WbWb$ with one W boson decaying leptonically and the other hadronically; CMS used final states where both, one or neither W decays leptonically and then combined the results. The $t\bar{t}$ invariant mass spectrum was analyzed for any excess, and no evidence for any resonance was seen. ATLAS excluded a narrow ($\Gamma/m = 1.2\%$) leptophobic top-color Z' boson with masses between 0.7 and 2.1 TeV and with $\Gamma/m = 3\%$ between 0.7 and 3.2 TeV. CMS set limits on leptophobic Z' bosons for three different assumed widths $\Gamma/m = 1.0\%$, $\Gamma/m = 10.0\%$, and $\Gamma/m = 30.0\%$ of 3.9 TeV to 4.0 TeV and exclude RS KK gluons up to 3.3 TeV.

Both ATLAS [74] and CMS [75] have also searched for resonances decaying into $q\bar{q}$, qg or gg using the dijet invariant mass spectrum. Excited quarks are excluded up to masses of 6.7 TeV and model-independent upper limits on cross sections with a gaussian signal shape were set. CMS excluded string resonances with masses below 7.9 TeV, scalar diquarks below 7.5 TeV, axigluons

and colorons below 6.6 TeV, excited quarks below 6.3 TeV, color-octet scalars below 3.7 TeV, W' bosons below 3.6 TeV, Z' bosons with SM-like couplings below 2.9 TeV and between 3.1 TeV and 3.3 TeV, Randall–Sundrum Gravitons below 2.6 TeV.

$W' \rightarrow \ell\nu$:

Both LHC experiments have also searched for massive charged vector bosons. In this section we include a summary of the results, with emphasis on final states with third generation fermions, while the details on other decays are discussed in the mini-review of W' [64]. ATLAS searched for a heavy W' decaying to $e\nu$ or $\mu\nu$ and find no excess over the standard model expectation. A sequential standard model (SSM) W' boson (assuming zero branching ratio to WZ) with mass less than 7 TeV was excluded [76] using 139 fb^{-1} dataset at $\sqrt{s} = 13$ TeV, as well as setting model independent cross-section limits as a function of mass. Based on a smaller dataset, the CMS experiment excluded a SSM W' boson with mass up to 4.1 TeV [77] and presented the upper limits on the production of generic W' bosons decaying into this final state using a model-independent approach.

CMS [78] has carried out a complementary search in the $\tau\nu$ final state. As noted above, such searches place limits on models with enhanced couplings to the third generation. No excess was observed and limits between 2.0 and 2.7 TeV were set on the mass of a W' decaying preferentially to the third generation; a W' with universal fermion couplings was also excluded for masses less than 2.7 TeV.

$W' \rightarrow t\bar{b}$:

Heavy new gauge bosons can couple to left-handed fermions like the SM W boson or to right-handed fermions. W' bosons that couple only to right-handed fermions (W'_R) may not have leptonic decay modes, depending on the mass of the right-handed neutrino. For these W' bosons, the $t\bar{b}$ ($t\bar{b} + \bar{t}b$) decay mode is especially important because in many models the W' boson is expected to have enhanced couplings to the third generation of quarks relative to those in the first and second generations. It is also the hadronic decay mode with the best signal-to-background. ATLAS and CMS have performed searches for W' bosons via the $W' \rightarrow t\bar{b}$ decay channel in the lepton+jets and all-hadronic final state.

The CMS lepton+jets search [79–82], $W' \rightarrow t\bar{b} \rightarrow Wbb \rightarrow \ell\nu bb$, proceeded via selecting events with an isolated lepton (electron or muon), and at least two jets, one of which is identified to originate from a b-quark. The mass of the W' boson ($M_{t\bar{b}}$) was reconstructed using the four-momentum vectors of the final state objects ($bb\ell\nu$). The distribution of $M_{t\bar{b}}$ is used as the search discriminant. A search [82] using 35.9 fb^{-1} of data, collected at $\sqrt{s} = 13$ TeV, led to an exclusion of W'_R bosons with masses below 3.4 TeV (3.6 TeV) if $M_{W'_R} \gg M_{\nu_R}$ ($M_{W'_R} < M_{\nu_R}$), where M_{ν_R} is the mass of the right-handed neutrino.

The CMS search for $W' \rightarrow t\bar{b}$ decays using the all-hadronic final state focused on W' masses above 1 TeV [81]. In this region, the top quark gets a large Lorentz boost and hence the three hadronic products from its decay merge into a single large-radius jet. Techniques which rely on substructure information of the jets [83] are employed to identify boosted all hadronic W boson and top quark jets and compute the mass of the jet. W' candidate mass was computed from back-to-back boosted top-tagged jet and a low mass b-tagged jet. From this all-hadronic search, W' bosons were excluded for masses up to 2.02 TeV.

ATLAS has searched for W'_R bosons in the $t\bar{b}$ final state both for lepton+jets [84] and all-hadronic [85] decays of the top. No significant deviations from the standard model were seen in either analysis and limits were set on the $W' \rightarrow t\bar{b}$ cross section times branching ratio and W' bosons with purely right-handed couplings to fermions were excluded for masses below 3.15 TeV when the two channels are combined.

In addition, the above studies also provided upper limits on the W' effective couplings to right- and left-handed fermions. In Fig. 93.1 (bottom) the upper limits on W' couplings normalized to the SM W boson couplings derived by ATLAS [86] are shown. The top panel of Fig. 93.1 shows the upper limits for arbitrary combinations of left- and right-handed couplings of the W' boson to fermions set using a model independent approach by CMS [82].

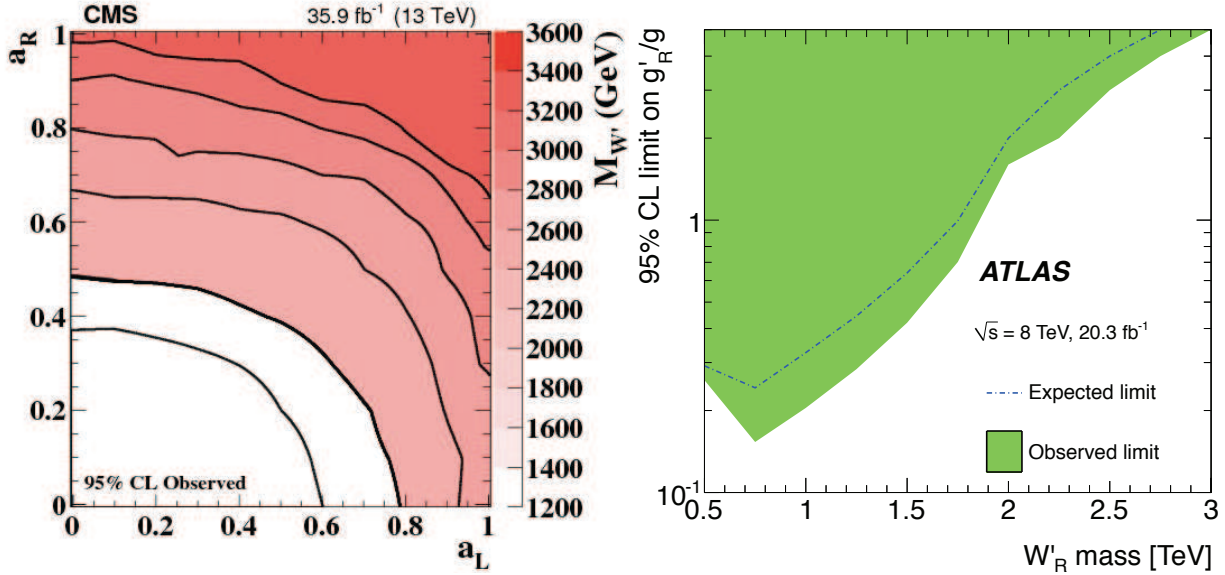


Figure 93.1: Left panel: Observed limits on the W' boson mass as function of the left-handed (a_L) and right-handed (a_R) couplings. Black lines represent contours of equal W' boson mass [82]. Right panel: Observed and expected regions, on the g'/g vs mass of the W' boson plane, that are excluded at 95% CL, for right-handed W' bosons [86].

93.2.2 Searches for Resonances decaying to Vector Bosons and/or Higgs Bosons

Both the ATLAS and CMS experiments have used the data collected at $\sqrt{s} = 13$ TeV to search for resonances decaying to pairs of bosons. Overall no significant excesses were seen in the full datasets that were analyzed and the results are interpreted in models with heavy vector triplets (HVT) [87], models with strong gravity and extra spatial dimensions, as well as setting model independent limits as a function of mass. For a full review of models including extra spatial dimensions including the interpretation of many of these results in that context please see the review of extra dimensions in this volume [60].

Utilizing data collected at $\sqrt{s} = 13$ TeV, ATLAS [88] and CMS [89], have both looked for a resonant state decaying into VV (with $V = W$ or Z), VH (with H representing the SM Higgs boson), and HH . Both collaborations have analyzed bosonic decay modes. ATLAS searches in the $qqqq$, $\nu\nu qq$, $lvqq$, $llqq$, $lv\nu\nu$, $ll\nu\nu$, $lvll$, $llll$, $qqbb$, $\nu\nu bb$, $lvbb$, and $llbb$ final states and combined the results (separately within each experiment). While CMS analyzes the $qqqq$, $\nu\nu qq$, $lvqq$, $llqq$, $ll\nu\nu$, $\nu\nu bb$, $lvbb$, $llbb$, $bbbb$, $\tau\tau bb$, and $qq\tau\tau$ final states.

The combined limits are expressed both as limits on the cross-section as a function resonance mass as well as constraints on the coupling of the heavy boson triplet to quarks, leptons, and the Higgs boson.

$X \rightarrow WZ$:

ATLAS searches for new heavy resonances decaying into WZ in the channels $WZ \rightarrow qqqq$ [90], $lvqq$ [91], and $lvll$ [92]. In the fully leptonic channel, the invariant mass of the WZ pair is obtained

by considering all possible four lepton permutations in each event. The dominant background is Standard Model continuum WZ production, ZZ production where one lepton is not identified or falls outside the detector acceptance, and top quark plus vector boson production. No resonant production is seen in data and lower limits on the mass of a HVT decaying into WZ are set at 2260 (2460) GeV assuming a coupling constant of $g_V = 1$ ($g_V = 3$). In the $WZ \rightarrow lvqq$ mode, ATLAS searches in both the cases that the quarks are observed as individual jets (resolved) and where they merge into one jet in the detector (boosted) which probe the low and high p_T regime of the Z boson. No significant excess is seen in either channel and combined lower mass limits are placed at 2900 (3000) GeV for $g_V = 1$ ($g_V = 3$) in the HVT model. In the all hadronic decay mode, ATLAS searches for two high p_T hadronically decaying vector bosons looking for a resonant structure. No excess is seen and limits are placed excluding 1200-3000 (1200-3300) GeV for $g_V = 1$ ($g_V = 3$) in the HVT model.

The CMS collaboration searches for $VV \rightarrow qq\bar{q}\bar{q}$ [93] in the large R dijet search. The W and Z boson are identified through the mass of the large R jet and substructure variables. No excess is seen and limits are set for charged HVT bosons with masses lower than 3200 (3800) GeV for $g_V = 1$ ($g_V = 3$). Cross-section limits as function of mass are reported for the charged spin-1 resonance interpretation and are placed at 44.4 fb at 1.4 TeV to 0.7 pb at 4 TeV. In the $\nu\nu qq$ final state [94], the CMS collaboration searches for a charged spin 1 resonance decaying into a VZ final state with a Z boson decaying into a pair of neutrinos and the other boson decaying into two collimated quarks reconstructed as a large R-jet. The transverse mass of the VZ candidate is reconstructed and utilized to search for evidence of resonant VZ production. No excess is seen and lower mass limits are placed on the charged resonance at 3100 (3400) GeV for $g_V = 1$ ($g_V = 3$). In the $2l2q$ final state, the CMS collaboration searches for a heavy resonance decaying into ZV [95] looking for events with one large R-jet consistent with the hadronic decay of a vector boson and a Z boson reconstructed in the charged lepton decay channel (e or μ). Limits are set for a HVT W' with a lower mass of 2270 (2330) for $g_V = 1$ ($g_V = 3$).

$X \rightarrow WW$:

The ATLAS collaboration searches for a new heavy resonance decaying into WW in the channels $WW \rightarrow qq\bar{q}\bar{q}$ [90], $lvqq$ [91], and $lv\nu$ [96]. In the case where both W s decay leptonically, ATLAS utilizes the transverse of the two lepton and two neutrino final state and searches for an excess in this distribution between 200 GeV and 5 TeV. No excess is seen and the mass of a HVT is excluded below 1300 GeV. Further vector boson fusion is also considered and cross-section limits as a function of mass are placed ranging from 1.3 pb to 0.006 pb at 200 GeV to 3 TeV, respectively. In the $lvqq$ mode, ATLAS completed a companion analysis to the $WZ \rightarrow$ analysis discussed above and places lower mass limits of 2850 (3150) GeV for $g_V = 1$ ($g_V = 3$) in the HVT model. ATLAS also interprets the all hadronic mode analysis in the hypothesis that $WW \rightarrow qq\bar{q}\bar{q}$ and places limits on a HVT boson decaying into WW in the all hadronic mode between 1200 to 2200 (1200 to 2800) GeV for $g_V = 1$ ($g_V = 3$).

The CMS collaboration searches for $VV \rightarrow qq\bar{q}\bar{q}$ [93] in the large R dijet search. The W and Z boson are identified through the mass of the large R jet and substructure variables. No excess is seen and limits are set for charged HVT bosons with masses lower than 2700 (2800) GeV for $g_V = 1$ ($g_V = 3$). Cross-section limits as function of mass are reported for the uncharged spin-1 resonance interpretation and are placed at 41.6 fb at 1.4 TeV to 0.6 pb at 4 TeV.

$X \rightarrow VH$:

The ATLAS Collaboration searches for a new heavy resonance decaying into WH and ZH in the $qqbb$ (WH and ZH) [97], $lvbb$ (WH), $\nu\nu bb$ (ZH), $lvbb$ (ZH) [98]. In the all hadronic mode,

ATLAS searches for boosted VH production looking for two large R jets where the larger invariant mass large R jet is interpreted as the Higgs boson decay products while the lesser the hadronically decaying vector boson requiring b tagging on the Higgs boson subjects. The invariant mass is reconstructed and a search is done for resonant production of ZH . None is found and limits from 1100 to 2500 (1300 to 3800 GeV) are placed for $g_V = 1$ ($g_V = 3$). ATLAS also searches for ZH where the W or Z boson decays into $\nu\nu$, $l\nu$, and ll . The analysis searches for both resolved and merged (boosted) b jets from the decay of the Higgs boson as well as defining signal regions based on the number of reconstructed charged leptons (0,1,or 2). In the dilepton channel the invariant mass is explicitly reconstructed of the entire diboson system, the single lepton channel reconstructs the diboson final state constraining the lepton and missing transverse momentum utilizing the known W boson mass, while the 0 charged lepton channel reconstructs the transverse mass of the diboson system. No excess is seen in any channel and limits on the production of a HVT are placed at 2800 GeV (2930) GeV for $g_V = 1$ ($g_V = 3$).

The CMS Collaboration searches for a heavy resonance decaying into VH [99] searching for resonances decaying into a Higgs boson and either a hadronically decaying W or Z boson. The search identifies events with two large-R jets using substructure variables and requires one large-R jets is tagged with a pair of b-hadrons clustered in a single jet. The invariant mass of the VH bosons is reconstructed and evidence for resonance production is sought. No excess is seen and limits are placed. With $g_V = 1$ (3) a narrow W' resonance with $m_{W'} < 2470(3150)$ GeV and $m_{Z'} < 1150(1190)$.
Summary of Searches with Diboson Final States:

Both ATLAS [88] and CMS [89] provide plots summarizing the various searches results and limits combining. The results are shown in the context of HVT models and models of strong gravity with extra spatial dimensions. No excess is seen in any search and limits on the 4.3 (4.5) TeV (ATLAS) and (CMS). Inclusion of decays directly to fermions increase these limits to 5.3 (5.5) TeV and 5.0 (5.2) TeV from the ATLAS and CMS combinations, respectively. Both collaborations also place varying limits on the coupling strength as a function of HVT boson mass as well.

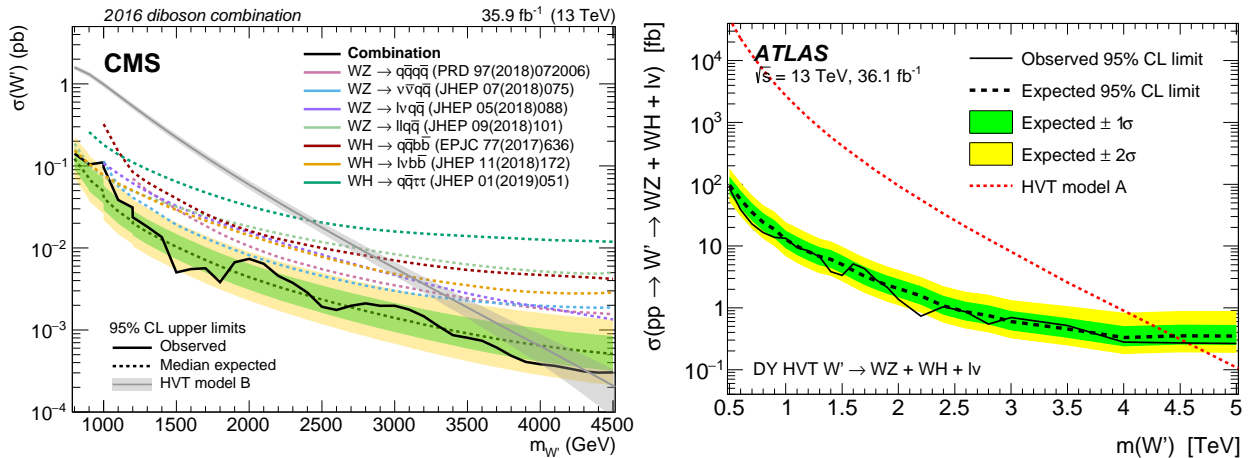


Figure 93.2: Left panel: Observed limits from W' to diboson from CMS [89]. Right panel: Observed limits from W' to diboson decays from ATLAS [88].

93.2.3 Vector-like third generation quarks

Vector-like quarks (VLQ) have non-chiral couplings to W bosons, i.e. their left- and right-handed components couple in the same way. They therefore have vectorial couplings to W bosons. Vector-like quarks arise in Little Higgs theories, top-color-models, and theories of a composite

Higgs boson with partial compositeness. In the following, the notation T quark refers to a vector-like quark with charge $2/3$ and the notation B quark refers to a vector-like quark with charge $-1/3$, the same charges as the SM top and b quarks respectively. The exotic vector-like quarks $X_{5/3}$ and $Y_{-4/3}$ have charges $5/3$, and $-4/3$ respectively. Vector-like quarks couple with SM quarks with Yukawa interactions and may exist as SU(2) singlets (T , and B), doublets $[(X_{5/3}, T), (T, B), (B, Y_{-4/3})]$, or triplets $[(X_{5/3}, T, B), (T, B, Y_{-4/3})]$. At the LHC, VLQs can be pair produced via the dominant gluon-gluon fusion. VLQs can also be produced singly by their electroweak effective couplings to a weak boson and a standard model quark. Single production rate is expected to dominate over the rate of pair production at large VLQ masses. T quarks can decay to bW , tZ , or tH^0 . Weak isospin singlets are expected to decay to all three final states with (asymptotic) branching fractions of 50%, 25%, 25%, respectively. Weak isospin doublets are expected to decay exclusively to tZ and to tH^0 [100] with equal branching ratios. Analogously, B quarks can decay to tW , bZ , or bH^0 . The $Y_{-4/3}$ and $X_{5/3}$ quarks decay exclusively to bW and to tW . While these are taken as the benchmark scenarios, other representations are possible and hence the final results are interpreted for many allowed branching fraction combinations.

Given the multiple decay modes of the VLQs, the final state signatures of both pair produced and the singly produced VLQs are fairly rich with leptons, jets, b jets, and missing energy. Depending on the mass of the VLQ, the top quarks and $W/Z/H^0$ bosons may be Lorentz boosted and identified using jet substructure techniques. Thus the searches are performed using lepton+jets signatures, multi-lepton and all-hadronic decays. In addition, T or B quarks with their antiparticles can result in events with same-sign leptons, for example if the decay $T \rightarrow tH \rightarrow bWW^+W^-$ is present, followed by leptonic decays of two same-sign W bosons. In the following subsections, while we describe the searches for each of the decay modes of the VLQs, the same analysis can be re-interpreted to obtain the sensitivity to a combination with varied branching fractions to the different decay modes.

In the following sections, the results obtained for T (B) quarks assuming 100% branching ratio to Wb (Wt) are also applicable to heavy vector-like $Y_{-4/3}$ ($X_{5/3}$) with charge $4/3$ ($5/3$).

93.2.3.1 Searches for T quarks that decay to W , Z and H^0 bosons

$T/Y \rightarrow bW$:

CMS has searched for pair production of heavy T quarks that decay exclusively to bW [101–103]. The analysis selected events with exactly one charged lepton, assuming that the W boson from the second T quark decays hadronically. Under this hypothesis, a 2-constraint kinematic fit can be performed to reconstruct the mass of the T quark as a narrow mass peak with a mass resolution of around 7%. In Refs. [102] and [103], the two-dimensional distribution of reconstructed mass vs S_T was used to test for the signal, where S_T is the scalar sum of the missing p_T and the transverse momenta of the lepton and the leading four jets. This analysis, when combined with the search in the fully hadronic final state [104] excluded new quarks that decay 100% to bW for masses below 0.89 TeV [103]. At times the hadronically-decaying W boson is produced with a large Lorentz boost, leading to the W decay products merged into a large-radius jet. Algorithms such as jet pruning [105] were used to remove contributions from soft, wide angle radiation, from large-radius jets, leading to better discrimination between QCD jets and those arising from decays of the heavy particles. If the mass of the boosted jet was compatible with the W boson mass, then the W boson candidate jet and its subjets were used in the kinematic reconstruction of the T quark. No excess over standard model backgrounds was observed. Upper limits on the production cross section as a function of the mass of T quarks were measured. By comparing them with the predicted cross section for vector like quark pair production, the strong pair production of T quarks was excluded for masses below 1.30 TeV (1.28 TeV expected) [101].

Another “cut-based” search for pair produced T quarks in the all-hadronic final state targeting the Wb decay mode [106], relies on mass reconstruction of two highest p_T Wb combinations using boosted W boson candidates with $p_T > 200$ GeV and b-tagged jets. H_T is used as the signal discriminator, with selected events divided into nine categories based on the multiplicity of W and b jets in the event. From this search T quarks with pure Wb decays are excluded for masses below 1.04 TeV (1.07 TeV expected).

An analogous search has been carried out by ATLAS [107,108] for the pair production of heavy T quarks. It used the lepton+jets final state with an isolated electron or muon and at least four jets, including a b jet and required reconstruction of the T quark mass. Given the mass range of the T quark being explored was from a 0.4 TeV to a couple of TeV, the W boson from the T quark may fall in two categories: those with a high boost leading to merged decay products, and others where the two jets from the W boson were resolved. In addition, the selection was optimized to require large angular separation between the high p_T W bosons and the b jets.

The $T \rightarrow Wb$ candidates were constructed from both the leptonically and hadronically decaying W bosons by pairing them with the two highest p_T b-tagged jets in the event. The pairing of b jets with W bosons which minimizes the difference between the masses of leptonically decaying T ($m_{lep}(T)$) and the hadronic T ($m_{had}(T)$) was chosen. Finally, $m_{lep}(T)$ was used as the discriminating variable in a signal region defined by high S'_T (here S'_T is defined as the scalar sum of the missing p_T , the p_T of the lepton and jets), and the opening angle between the lepton and the neutrino ($\Delta R(e, \nu)$). With the 36.1 fb^{-1} data collected during Run 2 at $\sqrt{s} = 13$ TeV, assuming 100% branching ratio to the Wb decay, the observed lower limit on the T mass was 1.35 TeV, and in the SU(2) singlet scenario, the lower mass limit was obtained to be 1.17 TeV [107].

A targeted search for a T quark, produced singly in association with a light flavor quark and a b quark and decaying into bW , was carried out by CMS at $\sqrt{s}=13$ teV and a dataset corresponding to 2.3 fb^{-1} [109]. The analysis used lepton+jets events, with at least one b-tagged jet with large transverse momentum, and a jet in the forward η region. Selected events were required to have $S''_T > 500$ GeV, where S''_T is defined as the scalar sum of the transverse momenta of the lepton, the leading central jet, and the missing transverse momentum. The invariant mass of the T candidate was used as the discriminating variable and was reconstructed using the four-vectors of the leptonically decaying W boson and the leading central jet. No excess over the standard model prediction was observed. As the VLQ width is proportional to the square of the coupling, upper limits were set on the production cross section assuming a narrow width VLQ with coupling greater than 0.5. For Y/T quarks with a coupling of 0.5 and a 100% branching fraction for the decay to bW the excluded masses were in the range from 0.85 to 1.40 TeV [109]. A similar search [110,111] performed by ATLAS singly produced T or $Y_{-4/3}$ quark decaying to Wb using a dataset corresponding to 36.1 fb^{-1} . The search was performed using lepton+jets events with a high p_T b-tagged jet, and at least one forward jet. The reconstructed mass of the $T/Y_{-4/3}$ quark, was used as the discriminating variable and showed no excess above the expectation from SM. Interference effects with the SM background are included in the study. This search led to 95% CL upper limits on the mixing angle $|\sin(\theta_L)|$ (C_L^{Wb}) in the range of 0.18–0.35 (0.25–0.49) for singlet T quark mass between 0.8–1.2 TeV. This search also provided limits as a function of the $Y_{-4/3}$ quark mass, on the coupling of the $Y_{-4/3}$ quark to bW , and the mixing parameter $|\sin\theta_R|$ (C_R^{Wb}) for a $(B, Y_{-4/3})$ doublet model [110]. For VLQ masses between 0.08–1.8 TeV, the limits on $|\sin(\theta_R)|$ (C_R^{Wb}) is in the range 0.17–0.55 (0.24–0.77), where limits on $|\sin\theta_R|$ are around 0.18–0.19 and below the constraints from electroweak precision observables for $Y_{-4/3}$ quark mass between 0.9–1.25 TeV. For $Y_{-4/3}$ quark in the triplets $(T, B, Y_{-4/3})$, limits on $|\sin(\theta_L)|$ (C_L^{Wb}) are between 0.16–0.39 (0.31–0.78) for masses between 0.8 GeV–1.6 TeV [110].

$T \rightarrow tH^0$:

ATLAS has performed a search for $T\bar{T}$ production with $T \rightarrow tH^0$ [108,112]. Given the dominant decay mode $H^0 \rightarrow b\bar{b}$, these events are characterized by a large number of jets, many of which are b jets. Thus the event selection required one isolated electron or muon and high jet multiplicity (including b-tagged jets). The sample is categorized by the jet multiplicity (5 and ≥ 6 jets in the 1-lepton channel; 6 and ≥ 7 jets in the 0-lepton channel), b tag multiplicity (2, 3 and ≥ 4) and mass-tagged jet multiplicity (0, 1 and ≥ 2). The distribution of m_{eff} , defined as the scalar sum of the lepton and jet p_T and the missing E_T , for each category were used as the discriminant for the final signal and background separation. No excess of events were found. Weak isospin doublet T quarks were excluded below 1.16 TeV.

A search by ATLAS for pair produced VLQs with an all-hadronic final state signature yields an exclusion of pure decays $T \rightarrow tH^0$ upto a T quark mass of 1.01 TeV [113]. This analysis used a deep neural network technique to identify jets originating from boosted bosons and top-quarks and described further in subsection 93.2.3.2.

The CMS search for $T\bar{T}$ production, with $T \rightarrow tH^0$ decays has been performed in both lepton+jets, multilepton and all-hadronic final states. The lepton+jets analysis [114] emphasizes the presence of large number of b-tagged jets, and combined with other kinematic variables in a Boosted Decision Tree (BDT) for enhancing signal to background discrimination. The multilepton analysis [114] was optimized for the presence of b jets and the large hadronic activity. For $\mathcal{B}(T \rightarrow Wb) = 1$, the combined lepton+jets and multilepton analyses led to a lower limit on T quark masses of 0.71 TeV. A search for $T \rightarrow tH^0$ in all-hadronic decays [115], optimized for a high mass T quark, and based on identifying boosted top quark jets has been carried out by CMS. This search aimed to resolve subjets within the jets arising from boosted top quark decays, including b tagging of the subjets. A likelihood discriminator was defined based on the distributions of H_T , and the invariant mass of the two b jets in the events for signal and background. No excess above background expectations was observed. Assuming 100% branching ratio for $T \rightarrow tH^0$, this analysis led to a lower limit of 0.75 TeV on the mass of the T quark.

Searches for T quarks at $\sqrt{s}=13$ TeV, based on a 2.6 fb^{-1} dataset [116] have been performed by CMS using the lepton+jets final state. This search has been optimized for high mass T quarks by exploiting techniques to identify W or Higgs bosons decaying hadronically with large transverse momenta. The boosted W channel excluded T quarks decaying only to bW with masses below 0.91 TeV, and the boosted tH channel excluded T quarks decaying only to tH for masses below 0.89 TeV.

A CMS search for $T \rightarrow tH^0$ with $H^0 \rightarrow \gamma\gamma$ decays has been performed [117] in pair production of T quarks. To identify the Higgs boson produced in the decay of the heavy T quark, and the subsequent $H^0 \rightarrow \gamma\gamma$ decay, the analysis focused on identification of two photons in events with one or more high p_T lepton+jets or events with no leptons and large hadronic activity. A search for a resonance in the invariant mass distribution of the two photons in events with large hadronic activity defined by the H_T variable showed no excess above the prediction from standard model processes. The analysis resulted in exclusion of T quark masses below 0.54 TeV.

A search for electroweak single production of T quark decaying to tH^0 using boosted topologies in fully hadronic [118] and lepton+jets [119] in the final states has been performed by CMS. The electroweak couplings of the T quarks to the SM third generation quarks are highly model dependent and hence these couplings determine the rates of the single T quark production. In both analyses, T quark candidate invariant mass was reconstructed using the boosted Higgs boson jets and the top quark. Higgs boson jets were identified using jet substructure techniques and subjet b tagging. For the lepton+jets analysis the top quark was reconstructed from the leptonically decaying W and the b jet, while in the all-hadronic analysis the top quark jet was tagged using substructure

analysis. There was no excess of events observed above background. Exclusion limits on the product of the production cross section and the branching fraction ($\sigma(pp \rightarrow Tqt/b) \times \mathcal{B}(T \rightarrow tH^0)$) were derived for the T quark masses in the range 0.70-1.8 TeV. From the lepton+jets analysis, for a mass of 1.0 TeV, values of ($\sigma(pp \rightarrow Tqt/b) \times \mathcal{B}(T \rightarrow tH^0)$) greater than 0.8 and 0.7 pb were excluded assuming left- and right-handed coupling of the T quark to standard model fermions, respectively [119]. For the all-hadronic analysis, upper limits between 0.31 and 0.93 pb were obtained on ($\sigma(pp \rightarrow Tqt/b) \times \mathcal{B}(T \rightarrow tH^0)$) for T quark masses in the range 1.0-1.8 TeV [118].

$T \rightarrow tZ$:

Both ATLAS and CMS searched for T quarks that decay exclusively into tZ in pp collisions at $\sqrt{s} = 13$ TeV. No excesses were found in either search.

ATLAS performed a search [120] for optimized pair production of vector-like top quarks decaying into tZ where the Z boson subsequently decays into neutrino pairs utilizing 36.1 fb^{-1} of data. The search selected events with one lepton, multiple jets, and significant missing transverse momentum. No significant excesses were found and lower limits on the mass of a vector like top quark were placed, excluding masses below 0.87 TeV (weak-isospin singlet), 1.05 TeV (weak-isospin doublet), and 1.16 TeV (pure tZ mode).

Another search by ATLAS for pair produced T decaying to tZ has been carried out by reconstructing the high transverse momentum Z boson from a pair of opposite-sign same-flavor lepton, using events with two or three charged leptons [121]. The final analysis is based on three final signatures. In the trilepton events, at least one b-tagged jet is required and S_T is used as the discriminating variable. In events with two leptons, at least 2 b jets are requested and those with zero or one high p_T top-tagged jet, use H_T as the discriminator. The second dilepton analysis with two top-tagged high p_T jets focuses on hadronically decaying heavy resonances and the invariant mass of the Z boson and the highest p_T b-tagged jet if found to be a good discriminating variable. No excess was observed over the background expectations. The combined analysis yields a lower limit on T quark mass of 1.03 TeV (1.21 TeV) in the singlet (doublet) model or 100% branching ratio for $T \rightarrow tZ$ a lower limit on the T quark mass of 1.34 TeV is obtained.

ATLAS has subsequently carried out a search [122] for singly produced T quark decaying to tZ where the Z boson decays into neutrino pairs. The search is carried out using 36.1 fb^{-1} of data in events with two different final state signatures: one with jets, and significant missing p_T (0L) and the other with single lepton, jets and missing p_T (1L). Events are divided into signal and dedicated W +jets and $t\bar{t}$ background control regions. The sensitivity to T quark signal is extracted using distributions of missing p_T for 1L and the distributions of transverse mass T quark constructed from missing p_T and the high p_T large-radius top-tagged jet for 0L analysis. There is no excess found over the expected background and lower limits on the production of T singlets is obtained as a function of the left- and right-handed couplings $c_{L,W}$ and $c_{R,W}$ to top quarks and W bosons, where c_W above 0.7 are excluded for T quark mass of 1.4 TeV. The limits on c_W are also recasted into expected and observed 95% CL upper limits for the mixing angle (θ_L) of a singlet T with the top quark.

CMS searched [123] for single production of T quarks decaying into tZ with the Z boson decaying to pairs of charged leptons (electrons and muons) and the top quark decaying hadronically using 35.9 fb^{-1} of data. Limits were placed on T quarks with masses between 0.7 and 1.7 TeV excluding the product of cross section and branching fraction above values of 0.27 to 0.04 pb. Additionally, limits on the product of cross section and branching fractions for a Z' boson decaying into tZ were set between 0.13 and 0.06 pb for Z' boson masses in the range from 1.5 to 2.5 TeV.

Similar searches by ATLAS for singly produced T decaying to Zt have been performed in final state signatures with two or three charged leptons [121]. The analysis relies on tagging b jets

and high p_T large-radius jets originating from top-quarks. Additional selections are devised to reduce the contributions from pair production of T quarks. For events with dilepton analysis, the discriminating variable is the mass of the T quark formed using the invariant mass of the Z boson candidate and the highest p_T top-tagged jet, while for the trilepton analysis, the variable S_T is used to search for an excess of data over the expected SM background. No excess above the SM expectations is observed. The two final states (dilepton and trileptons) are combined to obtain the final results. For the coupling parameter κ_T between 0.1–1.6, the 95% CL upper limits on the production cross section times branching fraction into Zt is between 0.16–0.18 (0.03–0.05) pb at T quark mass of 0.7 (2) TeV.

Combination of $T \rightarrow bW/tZ/tH^0$:

Most of the analyses described above targeted an individual decay mode of the T quark, with 100% branching ratio to either bW , tZ or tH^0 and were optimized accordingly. However, they have varied sensitivity to all three decay modes and the results can be interpreted as a function of branching ratios to each of the three decay modes, with the total adding up to unity ($\mathcal{B}(tH) + \mathcal{B}(tZ) + \mathcal{B}(Wb) = 1$).

Combinations of analyses have been performed by both ATLAS and CMS. The limits set by ATLAS searches in $W(\ell\nu)b = X$, $H(bb)b + X$, $Z(\nu\bar{\nu})$, $Z(\ell\ell)t/b + X$, dileptons with same-sign charge, trileptons, all-hadronic final states have been combined and the results obtained for various sets of branching fractions for T quark decays to bW , tH^0 and tZ are shown in Fig. 93.3 (left). In the combined analysis, ATLAS sets lower T quarks mass limit of 1.31 TeV for all possible values of the branching fractions to the three decay modes [107, 120, 124]. In Fig. 93.3, exclusion is shown in the plane of $\mathcal{B}(T \rightarrow Ht)$ versus $\mathcal{B}(T \rightarrow Wb)$, for different values of the T quark mass. The default branching ratio values for the weak-isospin singlet and doublet cases are also shown in Fig. 93.3 as yellow circle and star symbols respectively. Assuming a weak isospin (T, B) doublet and $|V_{Tb}| \ll |V_{tB}|$, T quark mass below 1.37 TeV is excluded.

CMS analysis for pair production of T , combined three channels with lepton final states: single lepton, two leptons with the same sign of the electric charge (SS), or at least three leptons (trilepton) [125]. For various combinations of branching fractions for T quark decays to bW , tH^0 and tZ , the combined results exclude T quarks with masses below 1.14–1.3 TeV and are shown in Figure 93.3 (right). Single lepton events are classified into 16 signal categories and 6 background control regions based on multiplicity of b-tagged, high p_T H^0 and W -tagged jets. The discriminating variables are H_T for H^0 -tagged and the minimum invariant mass constructed from the lepton and the b jet, $\min[M_{lb}]$, for zero H^0 -tagged events. For the same-sign dilepton and trilepton analyses, the non-prompt backgrounds due to misidentified jets and leptons are derived from data control regions. In the trilepton analysis the S_T variable is used as the signal discriminator binned in four categories based on the lepton flavor combinations (eee , $ee\mu$, $e\mu\mu$, $\mu\mu\mu$). The single lepton analysis is most sensitive for $tHbW$ and $WbWb$ decay modes, within the the SS dilepton analysis $tHtH$ and $tHtZ$ have the best efficiency and for trileptons the $tZtZ$ and $tHtZ$ decays modes have the highest efficiency. CMS excludes singlet (doublet) T quark masses below 1.2 (1.28) TeV. Masses below 800 GeV were excluded in previous searches. For T quark masses in the range 0.8–1.8 TeV, cross sections smaller than 30.4–9.4 fb (21.2–6.1 fb) are excluded for the singlet (doublet) scenario.

Another inclusive search for pair produced T in all-hadronic final state [106] has been performed by CMS using the boosted event shape tagger (BEST) neural network technique to classify jets in six categories W , Z , H^0 , t , b , and light. This search does not focus on a given VLQ mode, but on various combinations of the boson and quark jets in the final state. Anti- k_T jets with a distance parameter of 0.8 are used. The BEST NN algorithm simultaneously classifies jets according to heavy object type. For each of the six particle hypothesis, it boosts each jet constituent into corresponding

frame along jet momentum direction, and calculates event shape and angular variables in the boosted frame, with the expectation that when boosting to the correct rest frame, jet constituents will be isotropic and show the expected N-prong structure of the decaying object in its rest frame. A neural network is trained using the event shape and angular variables in the boosted frame to classify jets according to one of those six possibilities (W, Z, H, t, b, or light). The analysis bins the events into 126 categories depending on the number of W, Z, H, t, b, or light jets in the final state with a maximum of four such objects. For each category H_T^{AK8} , the scalar sum of p_T of all AK8 jets, is used as the signal discriminator. A scan over a combination of various branching fractions is also performed. This search excludes T quark masses in the range 0.74–1.37 TeV for the tH decay mode in the NN analysis.

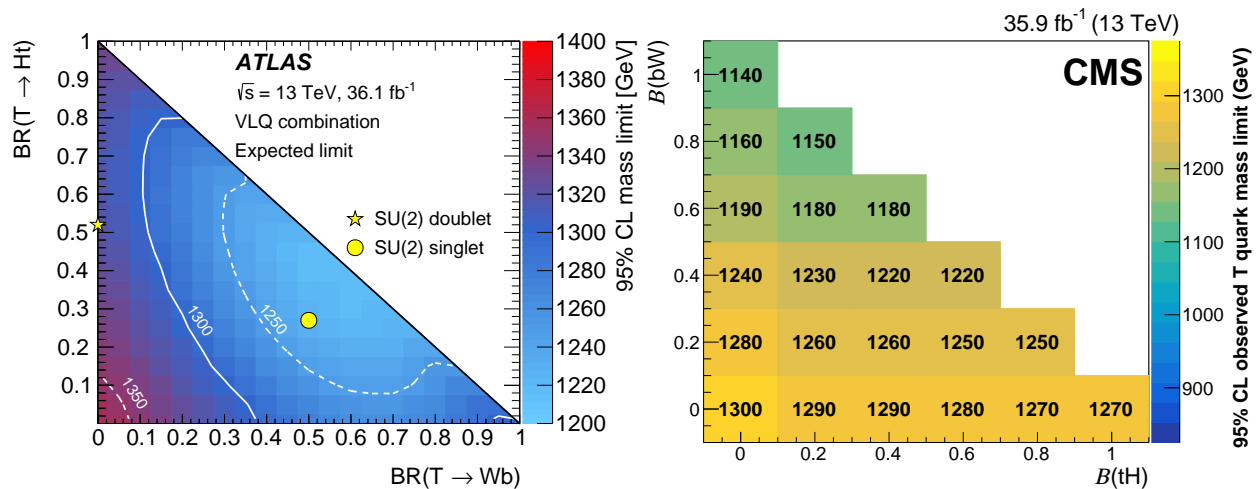


Figure 93.3: Left panel: observed limits on the mass of the T quark in the plane of $\mathcal{B}(T \rightarrow tH^0)$ versus $\mathcal{B}(T \rightarrow bW)$ from a combination [124] of all ATLAS searches for TT production. The markers indicate the default branching ratios for the SU(2) singlet and doublet scenarios. Right panel: the observed lower limits on the T quark mass (in GeV), from CMS searches after combining all lepton channels [125], for various branching fraction scenarios. $\mathcal{B}(T \rightarrow Wb) + \mathcal{B}(T \rightarrow tZ) + \mathcal{B}(T \rightarrow tH^0) = 1$ is assumed.

An inclusive search for VLQs has been carried out by CMS targeted at heavy T quarks decaying to any combination of bW , tZ , or tH^0 is described in [114]. Selected events have at least one isolated charged lepton. Events were categorized according to number and flavour of the leptons, the number of jets, and the presence of hadronic vector boson and top quark decays that are merged into a single jet. The use of jet substructure to identify hadronic decays significantly increases the acceptance for high T quark masses. No excess above standard model backgrounds was observed. Limits on the pair production cross section of the new quarks are set, combining all event categories, for all combinations of branching fractions into the three final states. For T quarks that exclusively decay to $bW/tZ/tH^0$, masses below 0.70/0.78/0.71 TeV are excluded.

93.2.3.2 Searches for B quarks that decay to W , Z and H^0 bosons

ATLAS and CMS have performed searches for pair production of heavy B quarks which subsequently decay to Wt , bZ or bH^0 . The searches have been carried out in final states with single leptons, dileptons (with same charge or opposite charge), multileptons, as well as in fully hadronic final states.

$B \rightarrow bH^0 X$:

Using 36.1 fb^{-1} of data, ATLAS has performed a search for pair produced VLQs with all-hadronic final state signature [113]. While this analysis provides exclusion limits for all third generation VLQs, it provides the strongest results for $B \rightarrow bH^0$ decay mode and excludes pure $B \rightarrow bH^0$ decays for B masses upto 1.01 TeV. The limits are also casted as a two-dimensional plane of branching ratio values of $B \rightarrow bH^0$ vs. $B \rightarrow Wb$. This analysis required the presence of high p_T jets and multiple b tags. It used a multi-class DNN to classify jets arising from W , Z , H^0 bosons and top-quarks. In addition, the matrix element method is used to compute the likelihood for the event to arise from a particular VLQ final state and used to construct the final discriminator. To increase the performance sensitivity, processes with the same number of top quarks, W/Z bosons, and H^0 Higgs bosons are combined into a single hypothesis.

 $B \rightarrow WtX$:

A search for $B \rightarrow tW$ in B pair produced events has been performed by the ATLAS experiment [107] using lepton+jets events with one hadronically decaying W and one leptonically decaying W utilizing 36.1 fb^{-1} of data at $\sqrt{s} = 13 \text{ TeV}$. The search was optimized for T production decaying into Wb . Since the analysis was optimized for $T \rightarrow Wb$ rather than Wt decays the analysis does not reconstruct the full B mass. As discussed earlier, the hadronically and leptonically decaying heavy quarks were required to have similar reconstructed masses (within 300 GeV). The interpretation of the $T \rightarrow Wb$ in the context of $B \rightarrow tW$ production led to the exclusion of heavy B like VLQs for masses less than 1.25 TeV and 1.08 TeV, assuming a 100% branching fraction to tW or SU(2) singlet B scenario, respectively.

A similar search by CMS [126], using 19.8 fb^{-1} of $\sqrt{s} = 8 \text{ TeV}$ data, selected events with one lepton and four or more jets, with at least one b-tagged jet, significant missing p_T , and further categorizes them based on the number of jets tagged as arising from the decay of boosted W , Z or H^0 bosons. The S_T distributions of the events in different categories showed no excess of events above the expected background and yielded a lower limit on the B quark mass of 0.73 TeV for $BR(B \rightarrow Wt) = 1$.

CMS [116] also searched for pair production of both TT and BB with collisions from 2.5 fb^{-1} of $\sqrt{s} = 13 \text{ TeV}$ data. The analysis searches for events with one high p_T lepton, multiple jets, and highly boosted W or Higgs bosons decaying hadronically. The analysis focuses on pair production and selects events with either a boosted W or Higgs candidate and then proceeds to search for anomalous production in excess of standard model production. Seeing no significant excesses CMS then proceeded to set limits in many different interpretations. The strongest was from the the $B \rightarrow Wt$ interpretation leading to excluding heavy vector-like B quark less than 0.73 TeV.

The all-hadronic inclusive analysis [106] performed by CMS using the BEST NN technique to classify $W/Z/H^0/t/b$ /light jets also gives exclusion limits on B quark production for various combinations of branching fractions for decays to tW , bZ , bH^0 . By considering categories based on various combinations of the boson and quark jets in the final state it excludes B quarks with masses up to 1230 GeV, for B decays to tW with a 100% branching fraction.

Electroweak production of single heavy $B+b$ productions has been studied by CMS in the decay to tW with lepton+jets final state [127]. Single lepton events with hadronic jets, including a forward jet, missing p_T are selected and divided into 10 different categories based on lepton flavor (e/μ), top-tagged, W -tagged, and 0/1/2 b -tagged jets. B quark mass m_{reco} is fully reconstructed from lepton, jets, and missing p_T , where the neutrino four-momentum is computed using the missing p_T and the W mass constraint (assuming massless ν). For events within top-tagged category, the high p_T top-tagged hadronic jet and the leptonically decaying W boson is used to compute m_{reco} . The m_{reco} distribution is used as the signal discriminator. In the absence of a excess over

the expected SM background, the exclusion limits on the production cross section is for B quark masses between 0.7-2 TeV varies between 0.3 to 0.03 pb. In addition, B quarks with left-handed couplings and a relative width of 10, 20, and 30% are excluded for masses below 1.49, 1.59, and 1.66 TeV respectively.

$B \rightarrow bZX$:

A search by CMS [128] for the pair-production of a heavy B quark and its antiparticle has been performed, where one the heavy B quark decays to bZ . Events with a Z boson decaying to e^+e^- or $\mu^+\mu^-$ and at least one b jet are selected. The signal from $B \rightarrow bZ$ decays are expected to appear as a local enhancement in the bZ mass distribution. No such enhancement was found and B quarks that decay 100% into bZ are excluded below 0.70 TeV. This analysis also set upper limits on the branching fraction for $B \rightarrow bZ$ decays of 30-100% in the B quark mass range 0.45-0.70 TeV. A complementary search has been carried out by ATLAS for new heavy quarks decaying into a Z boson and a b -quark [129]. Selected dilepton events contain a high transverse momentum Z boson that decays leptonically, together with two b jets. If the dilepton events have an extra lepton in addition to those from the Z boson, then only one b -jet is required. No significant excess of events above the standard model expectation was observed, and mass limits were set depending on the assumed branching ratios, as shown in Fig. 93.4. In a weak-isospin singlet scenario, a B quark with mass lower than 0.65 TeV was excluded, while for a particular weak-isospin doublet scenario, a B quark with mass lower than 0.73 TeV was ruled out.

ATLAS has searched for the electroweak production of single B quarks, which is accompanied by a b jet and a light jet [129]. The dilepton selection for double B production was modified for the single B production study by requiring the presence of an additional energetic jet in the forward region. An upper limit of 200 fb was obtained for the process $\sigma(pp \rightarrow B\bar{b}q) \times B(B \rightarrow Zb)$ with a heavy B quark mass at 0.70 TeV. This search indicated that the electroweak mixing parameter X_{Bb} below 0.5 is neither expected or observed to be excluded for any values of B quark mass.

Combination of $B \rightarrow tW/bZ/bH^0$:

The ATLAS experiment has combined the various analyses targeted for specific decay modes to obtain the most sensitive limits on the pair production of B quarks [107,108,124]. Various searches ($W(\ell\nu)t + X$, $Z(\ell\ell)t/b + X$, same sign charge dilepton events, trilepton events, and all-hadronic) are combined to obtain lower limits on the mass of the B quark in the plane of $BR(B \rightarrow Wt)$ vs $BR(B \rightarrow bH)$. The searches were optimized for 100% branching fractions and hence are most sensitive at large $BR(B \rightarrow Wt)$, and also at large $BR(B \rightarrow bH^0)$. For all possible values of branching ratios in the three decay modes tW , bZ , or bH^0 , the lower limits on the B quark mass was found to be 1.03 TeV and shown in Fig. 93.4 (left) as a function of both B mass and branching ratio.

CMS combined three channels with lepton final states: single lepton, two leptons with the same sign of the electric charge (SS), or at least three leptons (trilepton) [125]. For various combinations of branching fractions for B quark decays to tW , bH^0 and bZ , the combined results exclude b quarks with masses below 0.91–1.24 TeV and are shown in Figure 93.4 (right) the details are provided earlier in subsection 93.2.3.1. The single lepton analysis is most sensitive for $tHbW$ and $WbWb$ decay modes, within the the SS dilepton analysis $tHtH$ and $tHtZ$ have the best efficiency and for trileptons the $tZtZ$ and $tHtZ$ decays modes have the highest efficiency. CMS excludes singlet (doublet) B quark masses below 1.17 (0.94) TeV. Masses below 800 GeV were excluded in previous searches. For B quark masses in the range 0.8–1.8 TeV, cross sections smaller than 40.6–9.4 fb (101–49.0 fb) are excluded for the singlet (doublet) scenario.

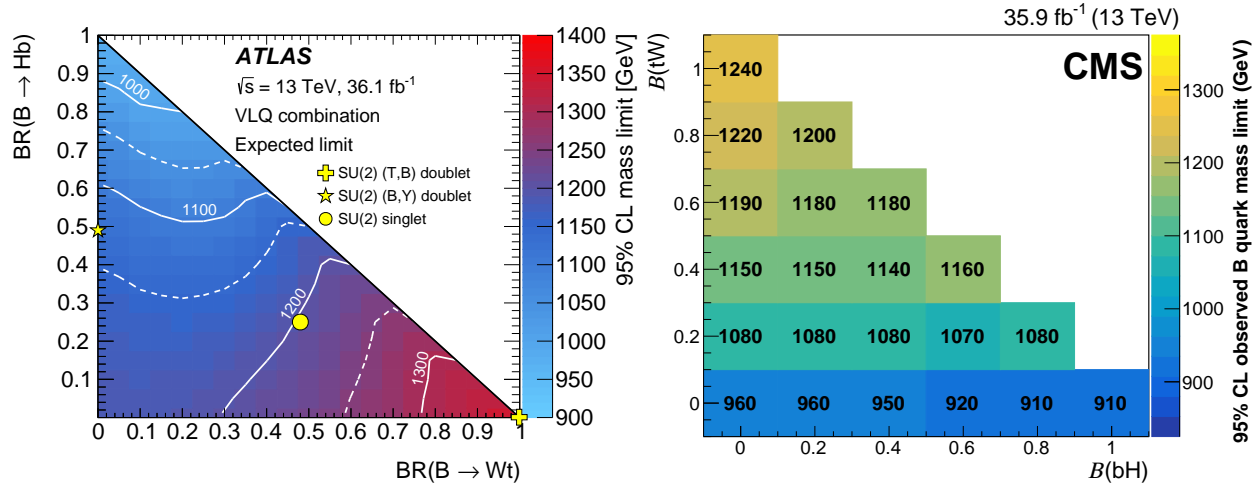


Figure 93.4: Observed limits on the mass of the B quark in the plane of $BR(B \rightarrow bH^0)$ versus $BR(B \rightarrow tW)$ from ATLAS searches [124] on the left panel, and CMS searches [125] on the right panel, for BB production. $B(B \rightarrow \mathcal{H}) + B(B \rightarrow \mathcal{Z}) + B(B \rightarrow \mathcal{W}\mathcal{L}) = 1$ is assumed. The yellow markers indicate the branching ratios for the SU(2) singlet and doublet scenarios.

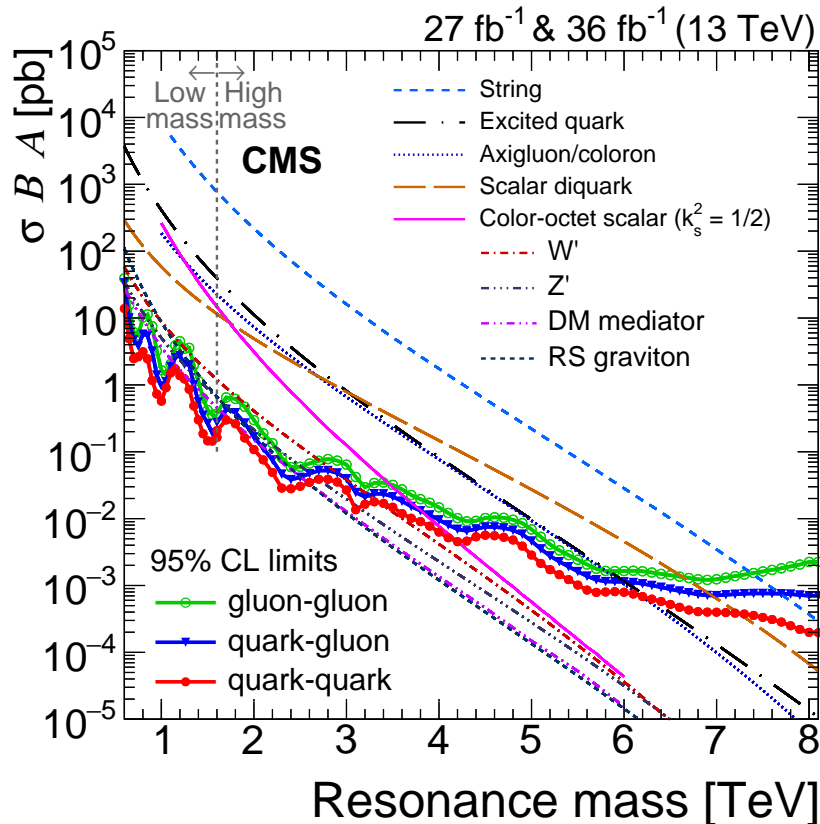


Figure 93.5: Observed 95% C.L. limits on $\sigma \times B \times A$ for string resonances, excited quarks, axigluons, colorons, E6 diquarks, s8 resonances, W' and Z' bosons, and Randall-Sundrum Gravitons g_{KK} from [130].

93.2.3.3 Searches for top-partner quark $X_{5/3}$

Searches for a heavy top vector-like quark $X_{5/3}$, with exotic charge $\pm 5/3$, such as that proposed in Refs. [131, 132], have been performed by both ATLAS and CMS [107, 133].

The analyses assumed pair-production or single-production of $X_{5/3}$ with $X_{5/3}$ decaying with 100% branching fraction to tW . Searches for $X_{5/3}$ have been performed using two final state signatures: same-sign leptons and lepton+jets.

The analysis based on searching for same-sign leptons, from the two W bosons from one of the $X_{5/3}$, has smaller backgrounds compared to the lepton+jets signature. Requiring same-sign leptons eliminates most of the standard model background processes, leaving those with smaller cross sections: $t\bar{t}$, W , $t\bar{t}Z$, WWW , and same-sign WW . In addition, backgrounds from instrumental effects due to charge misidentification were considered. Assuming pair production of $X_{5/3}$, the analyses by CMS using H_T as the discriminating variable restrict the $X_{5/3}$ mass to be higher than 1.16 (1.10) TeV for a right (left) handed chirality particle [133–135]. The limits obtained by ATLAS, by classifying the signal region by number of b jets, H_T , and missing p_T in the event, corresponded to a lower mass limit on $X_{5/3}$ of 1.19 TeV [136, 137].

Searches for $X_{5/3}$ using leptons+jets final state signatures are based on either full or partial reconstruction of the T mass from the lepton, jets (including b jets) and missing p_T . The CMS search [133, 138] also utilized jet substructure techniques to identify boosted $X_{5/3}$ topologies. The discriminating variable used was the mass constructed from the lepton and b-tagged jet, $M_{(\ell,b)}$, which corresponds to the visible mass of leptonically decaying top quark. To optimize the search sensitivity, the events were further separated into categories based on lepton flavor (e , μ), the number of b-tagged jets, the number of W-tagged jets, and the number of t-tagged jets. In the absence of a signal, the CMS analysis excluded $X_{5/3}$ quark masses with right-handed (left-handed) couplings below 1.32 (1.30) TeV [138]. Combining the lepton+jets with the same-sign leptons analyses leads to a slight improvement and excludes $X_{5/3}$ quark masses with right-handed (left-handed) couplings below 1.33 (1.30) TeV.

The ATLAS lepton+jets search for $X_{5/3}$ utilized events with high p_T W bosons and b jets. The search described earlier for T pair production, with $T \rightarrow Wb$ decays, can be reinterpreted as a search for $X \rightarrow tW$. This analysis excluded $X_{5/3}$ with masses below 1.25 TeV [107].

The single $X_{5/3}$ production cross section depends on the coupling constant λ of the tWX vertex. ATLAS has performed an analysis of same-sign dileptons which includes both the single and pair production. This analysis led to a lower limit on the mass of the $X_{5/3}$ of 0.75 TeV for both values of $\lambda = 0.5$ and 1.0 [139].

Single heavy $X_{5/3}+t$ production has been studied by CMS in the decay to tW with lepton+jets final state [127]. The description of the analysis is provided earlier in the discussion of $B \rightarrow WtX$ decays, where the reconstructed mass of $X_{5/3}$, m_{reco} distribution is used as the signal discriminator. In the absence of an excess over the expected SM background, the exclusion limits on the production cross section is for $X_{5/3}$ quark masses between 0.7–2 TeV varies between 0.3 to 0.03 pb, depending on the width of $X_{5/3}$ between 1–10%. In addition, $X_{5/3}$ quarks with left-handed couplings and a relative width of 10, 20, and 30% are excluded for masses below 0.92, 1.3, and 1.45 TeV respectively.

93.2.4 Heavy resonances decaying to VLQ

CMS has performed search for VLQ production in the decay of massive resonances such as Z' and W' bosons.

$Z' \rightarrow tT$: Specifically searches are presented by CMS in Refs. [140] and [141] for massive spin-1 Z' resonances decaying to a top quark and heavy VLQ top quark partner T . The results of this search for a heavy spin-1 resonance are interpreted in the context of two different models. In the G^* model which predicts ten VLQs (T , B , \tilde{T} , \tilde{B} , $T_{5/3}$, $T_{2/3}$, T' , B' , $B_{-1/3}$, $B_{-4/3}$) with the mass

relationship $M(T_{5/3}) = M(T_{2/3}) = M(T)\cos(\phi_L)$. For the benchmark scenario [142], $\cos(\phi_L)=0.84$ and the branching fractions $T \rightarrow tH^0, tZ, Wb$ are 0.25, 0.25 and 0.5 respectively. The ρ^0 model predicts a multiple of four new VLQs $T, B, X_{2/3}, X_{5/3}$, and in the benchmark scenario [143], the branching fractions $T \rightarrow tH^0, tZ, Wb$ are 0.5, 0.5 and 0 respectively.

Two of the three different decays of the $Z' \rightarrow tT$ with $T \rightarrow tH^0, tZ, Wb$ are characterized by the presence of two top quark decays and a boson (H^0/Z). A search [141] by CMS, optimized for $T \rightarrow tH/Zt$ decays is carried out in the lepton+jets final state using a dataset corresponding to an integrated luminosity of 35.9 fb^{-1} . Jet substructure techniques are used to identify (or tag) the high p_T large-radius jets originating from H^0, Z bosons and merged top quarks. The mass of the Z' boson is used as the signal discriminator and constructed using H^0 or Z -tagged dijet, the hadronic and leptonic top quark four vectors. For the leptonic top quark reconstruction ($t \rightarrow b\ell\nu_\ell$), the neutrino four vector is obtained from the event missing p_T using the W boson mass constraint. While the high p_T hadronic top quark jets from decays of massive Z' bosons are mostly merged and identified by top tagging techniques, those from T decays maybe resolved. The reconstructed Z' candidate events are classified into six different categories requiring the presence of either H^0 -tagged jet with 2 b-tagged subjets or one b-tagged subjet or a Z -tagged boson, each with either zero or one top-tagged jet. This search does not observe any significant deviation in data over the expectation from standard model backgrounds. Within the context of the G^* model, for a T mass of 1.2 (1.5), this search excludes G^* [142] resonances with masses between 1.5–2.3 (2.0–2.4) TeV.

The search in the all-hadronic final state is based on a 2.6 fb^{-1} dataset [140], and optimized for $T \rightarrow Wb$ decays. Jet substructure techniques are deployed for tagging jets from high p_T W boson and top quarks. Events are categorized into two groups based on the presence of b-tagged subjet in the top-tagged jet. Multijet background estimation is challenging and determined using side-bands defined by inverting the b tagging requirement. Upper limits on cross section for $Z' \rightarrow tT$ are obtained in the range of 0.13–10 pb. With additional data, this search has the potential to exclude scenarios in composite Higgs and extra dimension models.

$W' \rightarrow Tb/Bt$: W' bosons are predicted to decay to VLQ third generation partners T, B quarks within composite Higgs and warped extra dimensional models [144]. In the benchmark scenarios of this framework, W' decays to Tb or Bt are equally distributed and the subsequent VLQ decays $T \rightarrow tH$ and $B \rightarrow bH^0$ each are assumed to have a branching fraction of 0.5. The search for $W' \rightarrow Tb/bH^0 \rightarrow tbH^0$ is performed using a sample of 35.9 fb^{-1} by CMS [145] in the final state with all-hadronic decays of both the Higgs boson ($H^0 \rightarrow b\bar{b}$) and the top quark. Both the H^0 boson and the top quark are expected to be boosted in the decay of a heavy W' , and hence jet substructure techniques, including subjet b-tagging and double b-tagging are deployed to identify the H^0 -tagged and the top-tagged jets. The three particle mass m_{tbH^0} , is used as the signal discriminant to observe the W' resonance. There is no excess observed in data above the expected SM background. This search excludes W' production cross section above 0.01–0.43 pb for masses between 1.5–4.0 TeV.

93.2.5 Colorons and Colored Scalars

These particles are associated with top-condensate and top-seesaw models, which involve an enlarged color gauge group. The new particles decay to dijets, $t\bar{t}$, and $b\bar{b}$.

Direct searches for colorons, color-octet scalars and other heavy objects decaying to $q\bar{q}, qg, qg$, or gg has been performed using LHC data from pp collisions at $\sqrt{s}=7, 8$ and 13 TeV. Based on the analysis of dijet events from a data sample corresponding to a luminosity of 19.6 fb^{-1} , at $\sqrt{s}=8$ TeV the CMS experiment excluded pair production of colorons with mass between 1.20–3.60 and 3.90–4.08 TeV [146]. Analyses of inclusive 8- and 10-jet final states with low missing transverse momentum by CMS [147], set limits in several benchmark models. Colorons (axigluons) with masses between 0.6 and 0.75 (up to 1.15) TeV were excluded, and gluinos in R-parity violating

supersymmetric scenarios were ruled out from 0.6 up to 1.1 TeV.

A search for pair-produced colorons based on an integrated luminosity of 5.0 fb^{-1} at $\sqrt{s} = 7 \text{ TeV}$ by CMS excluded colorons with masses between 0.25 TeV and 0.74 TeV, assuming colorons decay 100% into $q\bar{q}$ [148]. This analysis was based on events with at least four jets and two dijet combinations with similar dijet mass. Color-octet scalars (s8) with masses between 1.20–2.79 TeV were excluded by CMS [146], and below 2.7 TeV by ATLAS [149].

These studies have now been extended to take advantage of the increased center-of-mass energy during Run 2 of the LHC. Using the 35.9 fb^{-1} of data collected at $\sqrt{s} = 13 \text{ TeV}$, searches for narrow resonances have been performed by CMS. An analysis of the dijet invariant mass spectrum formed using wide jets [130, 150, 151], separated by $\Delta\eta_{jj} \leq 1.3$, led to limits on new particles decaying to parton pairs (qq , qg , gg). Specific exclusions on the masses of colorons and color-octet scalars were obtained and are shown in Fig. 93.5. Exclusions have been obtained for axiglueons and colorons below 6.1 TeV, and color-octet scalars below 3.4 TeV.

93.3 Conclusions

As the above analyses have demonstrated, there is already substantial sensitivity to possible new particles predicted to accompany the H^0 in dynamical frameworks of electroweak symmetry breaking. No significant hints of any deviations from the standard model have been observed, and limits typically at the scale of a few hundred GeV to a few TeV are set.

Given the need to better understand the H^0 and to determine in detail how it behaves, such analyses continue to be a major theme of Run 2 the LHC, and we look forward to increased sensitivity as a result of the higher luminosity at the increased center of mass energy of collisions.

References

- [1] G. Aad *et al.* (ATLAS), Phys. Lett. **B716**, 1 (2012), [arXiv:1207.7214].
- [2] S. Chatrchyan *et al.* (CMS), Phys. Lett. **B716**, 30 (2012), [arXiv:1207.7235].
- [3] S. Weinberg, Physica **A96**, 1-2, 327 (1979).
- [4] A. Manohar and H. Georgi, Nucl. Phys. **B234**, 189 (1984).
- [5] H. Georgi, Nucl. Phys. **B266**, 274 (1986).
- [6] R. S. Chivukula, in “Flavor physics for the millennium. Proceedings, Theoretical Advanced Study Institute in elementary particle physics, TASI 2000, Boulder, USA, June 4-30, 2000,” 731–772 (2000), [hep-ph/0011264].
- [7] R. S. Chivukula, M. J. Dugan and M. Golden, Phys. Rev. **D47**, 2930 (1993), [hep-ph/9206222].
- [8] S. Weinberg, Phys. Rev. **D13**, 974 (1976), [Addendum: Phys. Rev.D19,1277(1979)].
- [9] L. Susskind, Phys. Rev. **D20**, 2619 (1979).
- [10] K. Lane (2002), [hep-ph/0202255].
- [11] C. T. Hill and E. H. Simmons, Phys. Rept. **381**, 235 (2003), [Erratum: Phys. Rept.390,553(2004)], [hep-ph/0203079].
- [12] R. Shrock, in “The origin of mass and strong coupling gauge theories. Proceedings, 5th International Workshop, SCGT’06, Nagoya, Japan November 21-24, 2006,” 227–241 (2007), [hep-ph/0703050].
- [13] E. Eichten *et al.*, Rev. Mod. Phys. **56**, 579 (1984), [Addendum: Rev. Mod. Phys.58,1065(1986)].
- [14] E. Eichten *et al.*, Phys. Rev. **D34**, 1547 (1986).
- [15] R. S. Chivukula and V. Koulovassilopoulos, Phys. Lett. **B309**, 371 (1993), [hep-ph/9304293].

- [16] R. Foadi, M. T. Frandsen and F. Sannino, Phys. Rev. **D87**, 9, 095001 (2013), [[arXiv:1211.1083](#)].
- [17] B. Holdom, Phys. Lett. **150B**, 301 (1985).
- [18] K. Yamawaki, M. Bando, and K.-i. Matumoto, Phys. Rev. Lett. **56**, 1335 (1986).
- [19] T. W. Appelquist, D. Karabali and L. C. R. Wijewardhana, Phys. Rev. Lett. **57**, 957 (1986).
- [20] T. Appelquist and L. C. R. Wijewardhana, Phys. Rev. **D35**, 774 (1987).
- [21] T. Appelquist and L. C. R. Wijewardhana, Phys. Rev. **D36**, 568 (1987).
- [22] E. Eichten, K. Lane and A. Martin (2012), [[arXiv:1210.5462](#)].
- [23] D. B. Kaplan and H. Georgi, Phys. Lett. **136B**, 183 (1984).
- [24] D. B. Kaplan, H. Georgi and S. Dimopoulos, Phys. Lett. **136B**, 187 (1984).
- [25] M. E. Peskin, Nucl. Phys. **B175**, 197 (1980).
- [26] J. Preskill, Nucl. Phys. **B177**, 21 (1981).
- [27] See “Status of Higgs Boson Physics” review in this volume.
- [28] R. Barbieri and A. Strumia, in “4th Rencontres du Vietnam: Physics at Extreme Energies (Particle Physics and Astrophysics) Hanoi, Vietnam, July 19-25, 2000,” (2000), [[hep-ph/0007265](#)].
- [29] N. Arkani-Hamed, A. G. Cohen and H. Georgi, Phys. Lett. **B513**, 232 (2001), [[hep-ph/0105239](#)].
- [30] N. Arkani-Hamed *et al.*, JHEP **08**, 020 (2002), [[hep-ph/0202089](#)].
- [31] N. Arkani-Hamed *et al.*, JHEP **07**, 034 (2002), [[hep-ph/0206021](#)].
- [32] M. Schmaltz and D. Tucker-Smith, Ann. Rev. Nucl. Part. Sci. **55**, 229 (2005), [[hep-ph/0502182](#)].
- [33] K. Agashe *et al.*, Phys. Lett. **B641**, 62 (2006), [[hep-ph/0605341](#)].
- [34] P. Sikivie *et al.*, Nucl. Phys. **B173**, 189 (1980).
- [35] B. Bellazzini, C. Csáki and J. Serra, Eur. Phys. J. **C74**, 5, 2766 (2014), [[arXiv:1401.2457](#)].
- [36] R. Essig *et al.*, JHEP **09**, 085 (2017), [[arXiv:1707.03399](#)].
- [37] Z. Chacko, H.-S. Goh and R. Harnik, Phys. Rev. Lett. **96**, 231802 (2006), [[hep-ph/0506256](#)].
- [38] R. S. Chivukula, A. G. Cohen and K. D. Lane, Nucl. Phys. **B343**, 554 (1990).
- [39] V. A. Miransky, M. Tanabashi and K. Yamawaki, Mod. Phys. Lett. **A4**, 1043 (1989).
- [40] W. A. Bardeen, C. T. Hill and M. Lindner, Phys. Rev. **D41**, 1647 (1990).
- [41] C. T. Hill, Phys. Lett. **B266**, 419 (1991).
- [42] B. A. Dobrescu and C. T. Hill, Phys. Rev. Lett. **81**, 2634 (1998), [[hep-ph/9712319](#)].
- [43] R. S. Chivukula *et al.*, Phys. Rev. **D59**, 075003 (1999), [[hep-ph/9809470](#)].
- [44] S. Dimopoulos and L. Susskind, Nucl. Phys. **B155**, 237 (1979), [[2,930\(1979\)](#)].
- [45] E. Eichten and K. D. Lane, Phys. Lett. **90B**, 125 (1980).
- [46] D. B. Kaplan, Nucl. Phys. **B365**, 259 (1991).
- [47] T. Appelquist, M. Piai and R. Shrock, Phys. Rev. **D69**, 015002 (2004), [[hep-ph/0308061](#)].
- [48] R.S. Chivukula, B.A. Dobrescu, and E.H. Simmons, Phys. Lett. **B401**, 74 (1997).
- [49] Y. Grossman and M. Neubert, Phys. Lett. **B474**, 361 (2000), [[hep-ph/9912408](#)].
- [50] S. J. Huber and Q. Shafi, Phys. Lett. **B498**, 256 (2001), [[hep-ph/0010195](#)].

- [51] T. Gherghetta and A. Pomarol, Nucl. Phys. **B586**, 141 (2000), [[hep-ph/0003129](#)].
- [52] K. Agashe, R. Contino and A. Pomarol, Nucl. Phys. **B719**, 165 (2005), [[hep-ph/0412089](#)].
- [53] G. F. Giudice *et al.*, JHEP **06**, 045 (2007), [[hep-ph/0703164](#)].
- [54] R. S. Chivukula and H. Georgi, Phys. Lett. **B188**, 99 (1987).
- [55] G. D’Ambrosio *et al.*, Nucl. Phys. **B645**, 155 (2002), [[hep-ph/0207036](#)].
- [56] K. Agashe *et al.* (2005), [[hep-ph/0509117](#)].
- [57] T. Appelquist and R. Shrock, Phys. Lett. **B548**, 204 (2002), [[hep-ph/0204141](#)].
- [58] K. Sakai, Nucl. Phys. **B867**, 429 (2013), [[arXiv:1207.4057](#)].
- [59] J. M. Maldacena, Int. J. Theor. Phys. **38**, 1113 (1999), [Adv. Theor. Math. Phys.2,231(1998)], [[hep-th/9711200](#)].
- [60] For a review, see C. Csaki, J. Hubisz, and P. Meade, [hep-ph/0510275](#) (2005), and “Extra Dimensions” review in this volume.
- [61] C. Pica, PoS **LATTICE2016**, 015 (2016), [[arXiv:1701.07782](#)].
- [62] T. Appelquist *et al.*, Phys. Rev. **D93**, 11, 114514 (2016), [[arXiv:1601.04027](#)].
- [63] PDG review on “ Z' -Boson Searches” in this volume.
- [64] PDG review on “ W' -Boson Searches” in this volume.
- [65] M. Aaboud *et al.* (ATLAS), Phys. Lett. **B**, 68 (2019), [[arXiv:1903.06248](#)].
- [66] CMS Collaboration, Technical Report CMS-PAS-EXO-19-019, CERN, Geneva (2019), URL <http://cds.cern.ch/record/2684757>.
- [67] G. Aad *et al.* (ATLAS), Phys. Rev. **D90**, 5, 052005 (2014), [[arXiv:1405.4123](#)].
- [68] M. Aaboud *et al.* (ATLAS), JHEP **01**, 055 (2018), [[arXiv:1709.07242](#)].
- [69] CMS Collaboration, JHEP **0217**, 48 (2017).
- [70] ATLAS Collaboration, ATLAS-CONF-2016-014 (2016).
- [71] CMS Collaboration, JHEP **0717**, 001 (2016).
- [72] M. Aaboud *et al.* (ATLAS), Phys. Rev. D. **99**, 092004 (2019), [[arXiv:1902.10077](#)].
- [73] A. M. Sirunyan *et al.* (CMS), JHEP **04**, 031 (2019), [[arXiv:1810.05905](#)].
- [74] ATLAS Collaboration, ATLAS-CONF-2019-007 (2019).
- [75] CMS Collaboration, CMS-PAS-EXO-19-012 (2019).
- [76] M. Aaboud *et al.* (ATLAS), Accepted by Phys. Rev. [[arXiv:1906.05609](#)].
- [77] V. Khachatryan *et al.* (CMS), Phys. Lett. **B770**, 278 (2017), [[arXiv:1612.09274](#)].
- [78] V. Khachatryan *et al.* (CMS), Phys. Lett. **B755**, 196 (2016), [[arXiv:1508.04308](#)].
- [79] S. Chatrchyan *et al.* (CMS), JHEP **05**, 108 (2014), [[arXiv:1402.2176](#)].
- [80] V. Khachatryan *et al.* (CMS), JHEP **02**, 122 (2016), [[arXiv:1509.06051](#)].
- [81] A. M. Sirunyan *et al.* (CMS), JHEP **08**, 029 (2017), [[arXiv:1706.04260](#)].
- [82] A. M. Sirunyan *et al.* (CMS), Phys. Lett. **B777**, 39 (2018), [[arXiv:1708.08539](#)].
- [83] CMS Collaboration, Technical Report CMS-PAS-JME-15-002, CERN, Geneva (2016), URL <http://cds.cern.ch/record/2126325>.
- [84] G. Aad *et al.* (ATLAS), Phys. Lett. **B788**, 347 (2019), [[arXiv:1807.10473](#)].
- [85] G. Aad *et al.* (ATLAS), Eur. Phys. J. **C75**, 4, 165 (2015), [[arXiv:1408.0886](#)].
- [86] G. Aad *et al.* (ATLAS), Phys. Lett. **B743**, 235 (2015), [[arXiv:1410.4103](#)].

- [87] D. Pappadopulo *et al.*, JHEP **09**, 060 (2014), [[arXiv:1402.4431](#)].
- [88] M. Aaboud *et al.* (ATLAS), Phys. Rev. **D98**, 5, 052008 (2018), [[arXiv:1601.04027](#)].
- [89] A. M. Sirunyan *et al.* (CMS), Phys. Lett. **B798**, 134952 (2019), [[arXiv:1906.00057](#)].
- [90] M. Aaboud *et al.* (ATLAS), Phys. Lett. **B**, 91 (2017), [[arXiv:1708.04445](#)].
- [91] M. Aaboud *et al.* (ATLAS), JHEP **03**, 042 (2018), [[arXiv:1710.07235](#)].
- [92] M. Aaboud *et al.* (ATLAS), Phys. Lett. **B**, 68 (2018), [[arXiv:1806.10532](#)].
- [93] A. M. Sirunyan *et al.* (CMS), Phys. Rev. **D97**, 072006, [[arXiv:1708.05379](#)].
- [94] A. M. Sirunyan *et al.* (CMS), JHEP **07**, 075, [[arXiv:1802.09407](#)].
- [95] A. M. Sirunyan *et al.* (CMS), JHEP **09**, 101, [[arXiv:1803.10093](#)].
- [96] M. Aaboud *et al.* (ATLAS), Eur. Phys. J. **C**, 78 (2017), [[arXiv:1710.01123](#)].
- [97] M. Aaboud *et al.* (ATLAS), Phys. Lett. **B**, 774 (2017), [[arXiv:1707.06858](#)].
- [98] M. Aaboud *et al.* (ATLAS), JHEP **B**, 174 (2018), [[arXiv:1712.06518](#)].
- [99] A. M. Sirunyan *et al.* (CMS), Eur. Phys. J. **C**, 636, [[arXiv:1707.01303](#)].
- [100] F. del Aguila *et al.*, Nucl. Phys. **B334**, 1 (1990).
- [101] A. M. Sirunyan *et al.* (CMS), Phys. Lett. **B779**, 82 (2018), [[arXiv:1710.01539](#)].
- [102] CMS Collaboration, Technical Report CMS-PAS-B2G-12-017 (2014).
- [103] V. Khachatryan *et al.* (CMS), Phys. Rev. **D93**, 1, 012003 (2016), [[arXiv:1509.04177](#)].
- [104] CMS Collaboration, Technical Report CMS-PAS-B2G-12-013 (2012).
- [105] S. D. Ellis, C. K. Vermilion and J. R. Walsh, Phys. Rev. **D80**, 051501 (2009), [[arXiv:0903.5081](#)].
- [106] A. M. Sirunyan *et al.* (CMS) (2019), [[arXiv:1906.11903](#)].
- [107] M. Aaboud *et al.* (ATLAS), JHEP **10**, 141 (2017), [[arXiv:1707.03347](#)].
- [108] G. Aad *et al.* (ATLAS), JHEP **08**, 105 (2015), [[arXiv:1505.04306](#)].
- [109] A. M. Sirunyan *et al.* (CMS), Phys. Lett. **B772**, 634 (2017), [[arXiv:1701.08328](#)].
- [110] M. Aaboud *et al.* (ATLAS), JHEP **05**, 164 (2019), [[arXiv:1812.07343](#)].
- [111] G. Aad *et al.* (ATLAS), Eur. Phys. J. **C76**, 8, 442 (2016), [[arXiv:1602.05606](#)].
- [112] ATLAS Collaboration (ATLAS), Technical Report ATLAS-CONF-2016-104 (2016).
- [113] M. Aaboud *et al.* (ATLAS), Phys. Rev. **D98**, 9, 092005 (2018), [[arXiv:1808.01771](#)].
- [114] S. Chatrchyan *et al.* (CMS), Phys. Lett. **B729**, 149 (2014), [[arXiv:1311.7667](#)].
- [115] V. Khachatryan *et al.* (CMS), JHEP **06**, 080 (2015), [[arXiv:1503.01952](#)].
- [116] A. M. Sirunyan *et al.* (CMS), JHEP **11**, 085 (2017), [[arXiv:1706.03408](#)].
- [117] CMS Collaboration, [cds.cern.ch/record/1709129](#) (2014).
- [118] A. M. Sirunyan *et al.* (CMS), JHEP **04**, 136 (2017), [[arXiv:1612.05336](#)].
- [119] V. Khachatryan *et al.* (CMS), Phys. Lett. **B771**, 80 (2017), [[arXiv:1612.00999](#)].
- [120] M. Aaboud *et al.* (ATLAS), JHEP **08**, 052 (2017), [[arXiv:1705.10751](#)].
- [121] M. Aaboud *et al.* (ATLAS), Phys. Rev. **D98**, 11, 112010 (2018), [[arXiv:1806.10555](#)].
- [122] M. Aaboud *et al.* (ATLAS), JHEP **05**, 041 (2019), [[arXiv:1812.09743](#)].
- [123] A. M. Sirunyan *et al.* (CMS), Phys. Lett. **B781**, 574 (2018), [[arXiv:1708.01062](#)].
- [124] M. Aaboud *et al.* (ATLAS), Phys. Rev. Lett. **121**, 21, 211801 (2018), [[arXiv:1808.02343](#)].

- [125] A. M. Sirunyan *et al.* (CMS), JHEP **08**, 177 (2018), [[arXiv:1805.04758](#)].
- [126] CMS Collaboration, Technical Report CMS-PAS-B2G-12-019 (2012).
- [127] A. M. Sirunyan *et al.* (CMS), Eur. Phys. J. **C79**, 90 (2019), [[arXiv:1809.08597](#)].
- [128] V. Khachatryan *et al.* (CMS), Phys. Rev. **D93**, 11, 112009 (2016), [[arXiv:1507.07129](#)].
- [129] G. Aad *et al.* (ATLAS), JHEP **11**, 104 (2014), [[arXiv:1409.5500](#)].
- [130] A. M. Sirunyan *et al.* (CMS), JHEP **08**, 130 (2018), [[arXiv:1806.00843](#)].
- [131] R. Contino and G. Servant, JHEP **06**, 026 (2008), [[arXiv:0801.1679](#)].
- [132] J. Mrazek and A. Wulzer, Phys. Rev. **D81**, 075006 (2010), [[arXiv:0909.3977](#)].
- [133] A. M. Sirunyan *et al.* (CMS), JHEP **08**, 073 (2017), [[arXiv:1705.10967](#)].
- [134] CMS Collaboration, Technical Report CMS-PAS-B2G-16-019 (2017).
- [135] S. Chatrchyan *et al.* (CMS), Phys. Rev. Lett. **112**, 17, 171801 (2014), [[arXiv:1312.2391](#)].
- [136] M. Aaboud *et al.* (ATLAS), JHEP **12**, 039 (2018), [[arXiv:1807.11883](#)].
- [137] G. Aad *et al.* (ATLAS), Phys. Rev. **D91**, 11, 112011 (2015), [[arXiv:1503.05425](#)].
- [138] A. M. Sirunyan *et al.* (CMS), JHEP **03**, 082 (2019), [[arXiv:1810.03188](#)].
- [139] G. Aad *et al.* (ATLAS), JHEP **10**, 150 (2015), [[arXiv:1504.04605](#)].
- [140] A. M. Sirunyan *et al.* (CMS), JHEP **09**, 053 (2017), [[arXiv:1703.06352](#)].
- [141] A. M. Sirunyan *et al.* (CMS), Eur. Phys. J. **C79**, 3, 208 (2019), [[arXiv:1812.06489](#)].
- [142] C. Bini, R. Contino and N. Vignaroli, JHEP **01**, 157 (2012), [[arXiv:1110.6058](#)].
- [143] D. Greco and D. Liu, JHEP **12**, 126 (2014), [[arXiv:1410.2883](#)].
- [144] N. Vignaroli, Phys. Rev. **D89**, 9, 095027 (2014), [[arXiv:1404.5558](#)].
- [145] A. M. Sirunyan *et al.* (CMS), JHEP **03**, 127 (2019), [[arXiv:1811.07010](#)].
- [146] V. Khachatryan *et al.* (CMS), Phys. Rev. **D91**, 5, 052009 (2015), [[arXiv:1501.04198](#)].
- [147] V. Khachatryan *et al.* (CMS), Phys. Lett. **B770**, 257 (2017), [[arXiv:1608.01224](#)].
- [148] S. Chatrchyan *et al.* (CMS), Phys. Rev. Lett. **110**, 14, 141802 (2013), [[arXiv:1302.0531](#)].
- [149] G. Aad *et al.* (ATLAS), Phys. Rev. **D91**, 5, 052007 (2015), [[arXiv:1407.1376](#)].
- [150] A. M. Sirunyan *et al.* (CMS), Phys. Lett. **B769**, 520 (2017), [Erratum: Phys. Lett. **B772**, 882(2017)], [[arXiv:1611.03568](#)].
- [151] CMS Collaboration, Technical Report CMS-PAS-EXO-15-001 (2015).